Thermo II Group Project

Phil Mai, Jayden Nelson, Hoonbae Park, Ali Ukperaj

Chemical Engineering Thermodynamics II 14:155:309

November 21, 2023

Table of Contents

Introduction and Background 3

Methods 5

Results and Discussion 10

- **Changing Pressure Plots** 11
- **Changing Temperature Plots** 13
- **Changing Composition Plots** 16
- **Discussion** 18

Conclusion 20

Works Cited 22

Introduction and Background

Gasification is a conversion process that takes a carbon-based material at a high temperature (>700°C) and turns it into a mixture of gases (typically CO, H_2, and CO_2). Synthesis gas (syngas) is a vapor mixture composed mainly of CO and H_2 and is a common product of the above process. It is produced using carbon-rich feedstocks such as coal, biomass, and other waste materials through gasification. Other components of syngas are carbon dioxide (CO_2) and methane (CH_4) in trace amounts; these values are often dependent on the ratio of CO and H_2 in the reaction.

A primary function of synthetic gas is as an intermediate or precursor to other chemical fuels, such as gasoline and paraffins. Syngas undergoes this change through Fischer-Tropsch synthesis (FTS), a catalyzed reaction that turns synthetic gas (reactants are CO and H_2) into a multitude of straight chain hydrocarbons (1 carbon to 100+) (Guilera et al., p. 1). The variety of alkanes produced typically depends on the thermodynamics and kinetics of the reaction, and secondary products such as alkenes and alcohols are also formed from this dependence (Mahmoudi et al. 15). Typical catalysts are either iron based – a fundamental component in the reaction to produce H_2O and remove CO_2 (Mahmoudi et al., p. 17) – or based on lesser known transition metals (cobalt, ruthenium, etc). The use of syngas in this manner is important in the context of today's global climate; alternative methods to produce fuels in a cleaner fashion are sorely needed to lower greenhouse gas emissions and tamper the effects of climate change.

As a renewable energy source, synthesis gas can be used to replace other commonly used fuels. Syngas is typically produced from biomass – matter from recently living organisms (carbon-based). Unlike fossil fuels, biomass is a renewable energy source, as it is continually produced and replenished over a short time period. This biomass can be converted into

electricity, heat, and other fuels that are used as reliable energy sources (Thomson et al., p. 21089). Biomass typically undergoes gasification for conversion into syngas, making biomass gasification a major process used around the world to produce clean energy.

Besides biomass, multiple alternative syngas pathways have been created as a clean source of energy. Carbon capture and utilization (CCU) is a process by which CO_2 is captured from industrial processes and stored for use in other industrial processes. Although syngas is composed mainly of CO and H_2, it contains a small amount of CO_2, which could cause pollution to the environment. By utilizing a CCU process and a catalyst such as CaO or $CaCO_3$, syngas can be nearly purified (>75% conversion) (Sun et al., p. 1). Other additional techniques, such as using gas runoff from mill gases as feedstock could be used as well.

Despite its numerous uses, syngas should be handled carefully, as it is a very hazardous material when released at large. Syngas contains carbon monoxide, which is a toxic, odorless material. CO easily binds to hemoglobin, reducing cellular respiration, which can quickly cause breathing problems and damage to the central nervous system (Stolecka & Rusin, p. 2537). Additionally, the main components of syngas and its trace elements are all flammable; as such, the combination will also be very flammable. Immediate ignition can cause jet fires and explosions, which pose threats to the environment (Stolecka & Rusin, p. 2540).

Based on the above, studying the mixture of H_2 and CO as synthetic gas is very important for future developments. Any research or new discoveries done on syngas can be used to extract it more efficiently, use it more efficiently, and clean it up more efficiently. Thermodynamically, analyzing how the compound should behave ideally and how it deviates from ideality can be used to isolate the specific system conditions where the mixture would be safe to extract and use.

Methods

To observe the fugacity coefficients of the H_2 and CO binary mixture as a function of pressure, temperature, and composition, we utilized MATLAB and equation of state methods of finding fugacity. Specifically, we used the Van der Waals EOS; our components are fairly simple molecules, and as such, we believed that a simpler EOS would be appropriate to use.

To utilize the Van der Waals equation, we first located critical temperatures and pressures of H_2 and CO (from Appendix A.1.2 of Koretsky) and inputted them into the MATLAB code. These critical data were then used to compute the a and b parameters for the two different components. The equations for finding a and b are as follows:

$$a = \frac{27(RT_c)^2}{64P_c}$$

$$b = \frac{RT_c}{8P_c}$$

These equations are well known, but for clarity they can be found in Koretsky as equations 4.21 and 4.22. With this, we also assumed a basis of 10 moles to help simplify our calculations involving mole fractions; this value is arbitrary and any number of total moles could be picked for our process.

To clearly see a correlation in changing the variables, a range of pressure and temperature values were chosen to test for. Pressures ranged from 12,000 Pa to 10,000,000 Pa and temperatures ranged from 10 K to 650 K. In MATLAB, the linspace function generates an array of evenly spaced points between a specified starting point and ending point. Using this function, 50 data points with equal increments within the temperature and pressure ranges were generated. With these pressure and temperature values, the relative pressure and relative temperature data were generated using the respective critical values of H_2 and CO.

After generating a set of 50 pressure and 50 temperature values, the corresponding specific volume data for H_2 and CO were found using a combination of each pressure and temperature data. It was assumed that the compositions of H_2 and CO in the mixture does not have any impact on the volume. To generate the specific volume data set, a nested loop was created, where the outside loop would access each of the pressure values, and the inside loop would access the temperature values. Then the fsolve command was run on the Van der Waals equation of state to solve for the volume of each component at its respective temperature and pressure. In MATLAB, the fsolve function is used to solve for a specific variable in the form f(x) = 0. The Van der Waals equation of state used to solve for volume is as follows:

$$P - \frac{RT}{v-b} - \frac{a}{v^2} = 0$$

To account for the 50 data points of pressure and temperature, 50 mole fractions for H_2 and CO were generated from a range of 0 to 1. Since the sum of the two compositions always equals 1 for a binary mixture, compositions of H_2 were simply generated by subtracting the composition of CO from 1. With each of the compositions, the values for a_{mix} and b_{mix} were calculated. The equations for finding a_{mix} and b_{mix} are as follows:

$$a_{mix,f} = y_1^2 a_1 + y_2^2 a_2 + 2y_1 y_2 a_{12}$$

$$b_{mix} = y_1 b_1 + y_2 b_2$$

These are found as equations 4.36 and 4.39 in Koretsky. An additional $a_{mix,f}$ term was calculated. This consists of a collection of terms found next to “Species 1 in a binary mixture” in Table 7.1 of Koretsky:

$$a_{mix,f1} = y_1 a_1 + y_2 a_{12}$$

$$a_{mix,f2} = y_2 a_2 + y_1 a_{12}$$

This term was created for (1) simplification of the equation used later to calculate the fugacity coefficient of both compounds and (2) its similarity to a_{mix} listed above. In terms of the binary mixing parameter (k_{12}), we decided to neglect it. This is because we found that a_1 and a_2 were similar enough to where a correction factor wouldn't be necessary. As such, we calculated a_{12} from equation 4.37 in Koretsky, which is:

$$a_{12} = \sqrt{a_1 a_2}$$

Using all of the information above, we then created a function to calculate the fugacity coefficients of CO and H_2 for each of the scenarios listed under Question 2. These are listed below:

1. Pressure (at constant temperature and composition)
2. Temperature (at constant pressure and composition)
3. Composition (at constant pressure and temperature)

This function calculated both the natural log (ln) and base log ($\log_{10}$) of the fugacity coefficient for both components given each of the above conditions. This calculation was run for several isotherms and isobars (these lines are specified as different T_r and P_r values). In order to calculate the base logs of the fugacity coefficients, Table 7.1 in Koretsky was used, specifically, the VdW EOS for species 1 in a binary mixture:

$$ln(\widehat{\phi_1}) = \frac{b_1}{v-b_{mix}} - ln(\frac{(v-b)P}{RT}) - \frac{2a_{mix,f}}{RTv}$$

Once calculated, $\log_{10}(\phi)$ was plotted against y_1, y_2, T_r, and P_r for both H_2 and CO. Plots are depicted in the **<u>Results and Discussion</u>** section.

Next, we used the Lee-Kesler equation of state to solve for the pure species fugacity coefficient and pure species fugacity at two different temperature and pressure compositions that

matched up with data found in the previous section. The Lee-Kesler equation of state (7.11 in Koretsky) is shown below:

$$log\phi_i = log\phi^{(0)} + \omega log\phi^{(1)}$$

To test the accuracy of this model, we used one point in ideal conditions and one point in non-ideal conditions. For CO, our ideal point was at a reduced pressure of 0.295 (10.312 x 10^5 Pa) and a reduced temperature of 2.1391 (284.286 K). The non-ideal point for CO was at a reduced pressure of 1.4611 (5.10792 x 10^6 Pa) and a reduced temperature of 0.5666 (75.31 K). For H_2, we initially ran into problems when finding ideal and non-ideal coordinates. Since we're ultimately utilizing data from Koretsky, we need reduced values that are either tabulated in Appendicies C.7 and C.8 or that can be interpolated using data from C.7 and C.8. Koretsky tabulates the Lee-Kesler data with P_r ranging from 0.01 - 10 and T_r ranging from 0.3 - 5. Although the pressures and temperatures above will give us reduced values for CO that fit within these ranges, the ideal point will give us a reduced temperature of over 8 for H_2 – due to its exceptionally low critical temperature (33.2 K). Therefore, a different point was used to measure our ideal fugacity of H_2: a reduced pressure of 0.1664 (2.158 x 10^6 Pa) and a reduced temperature of 3.84 (127.55 K). The non-ideal point for H_2 used the same pressure and temperature as CO, but now with a P_r of 3.9383 and a T_r of 2.2683.

These values are within the range of the Lee-Kesler data, but not matched perfectly with the indices, so double interpolation is needed for all 4 points (ideal and non-ideal points for CO and H_2). For the following discussion, consider the reduced pressures and temperatures from the appendix that are below our reference values as P_{low} and T_{low}, our actual values as P_r and T_r,and the values above our reference values as P_{high} and T_{high}.

In order to double interpolate, we recorded values of $log\phi^{(0)}$ and $log\phi^{(1)}$ at combinations of [P_{low}, T_{low}], [P_{low}, T_{high}], [P_{high}, T_{low}], and [P_{high}, T_{high}]. Next, we wrote an interpolation formula in MATLAB that calculated the value of $log\phi^{(0)}$ or $log\phi^{(1)}$ we were looking for (which is set as y in the equation). This function takes inputs of y_{low}, y_{high}, x_{low}, x, and x_{high} as listed below:

$$y = y_{low} + (y_{high} - y_{low})(\frac{x - x_{low}}{x_{high} - x_{low}})$$

The first interpolation was done to find $log\phi^{(0)}$ and $log\phi^{(1)}$ values at a constant P_{low} and our T_r (P_{low}, T_r) by using our function between $log(\phi)$ at (P_{low}, T_{low}) and $log(\phi)$ (P_{low}, T_{high}). We then interpolated between $log(\phi)$ at (P_{high}, T_{low}) and (P_{high}, T_{high}) to get a value at (P_{high}, T_r). Finally, interpolating between these two derived values gets us values of $log\phi^{(0)}$ and $log\phi^{(1)}$ at (P_r, T_r). This process was replicated for both CO and H_2 ($log\phi^{(0)}$ and $log\phi^{(1)}$) at the ideal and non-ideal points chosen above, giving us 4 sets of ($log\phi^{(0)}$, $log\phi^{(1)}$) values. These values, along with the acentric factor (ω) were plugged into the Lee-Kesler equation of state.

With the fugacity coefficient for each point of interest, we were able to match these values to their respective reduced values and plot points of $log(\phi)$ as functions of both pressure and temperature.

Results and Discussion

In order to plot the log of the fugacity coefficients with respect to each independent variable (pressure, temperature, and composition), each line must include one changing variable and two constant variables. The easiest way to create the plots was to take the values of $log(\phi)$ over a range of one independent variable (while keeping the other non-changing variable constant) and plotting across multiple values for the third, dependent variable.

For example, for our graphs of changing pressures, we plotted P_r vs $log(\phi)$ for 13 isotherms (so a range of 13 different temperatures) at one composition (same y_i for each isotherm). In order to provide a greater range of data, we repeated the above process for a second composition. The mole fractions chosen are arbitrary; we found that picking a composition where CO is around ⅓ of the mixture and another where it's around ⅔ of the mixture would be appropriate for showing how $log(\phi)$ varies at different conditions.

With two components, we had four graphs of P_r vs $log(\phi)$ with 13 isotherms plotted: two for CO where $y_{CO} = 0.3061$ and $y_{CO} = 0.6939$, and two for H_2 where $y_{H2} = 0.6939$ and $y_{H2} = 0.3061$. This procedure is identical for changing temperatures, where P_r is switched with T_r and isotherms are replaced with isobars. For composition we followed the same outline and decided to plot $log(\phi)$ over a range of temperatures (13 isotherms) at two different pressures (held constant): 2.2542×10^6 Pa for the first two graphs and 5.107918×10^6 Pa for the last two graphs.

Changing Pressure

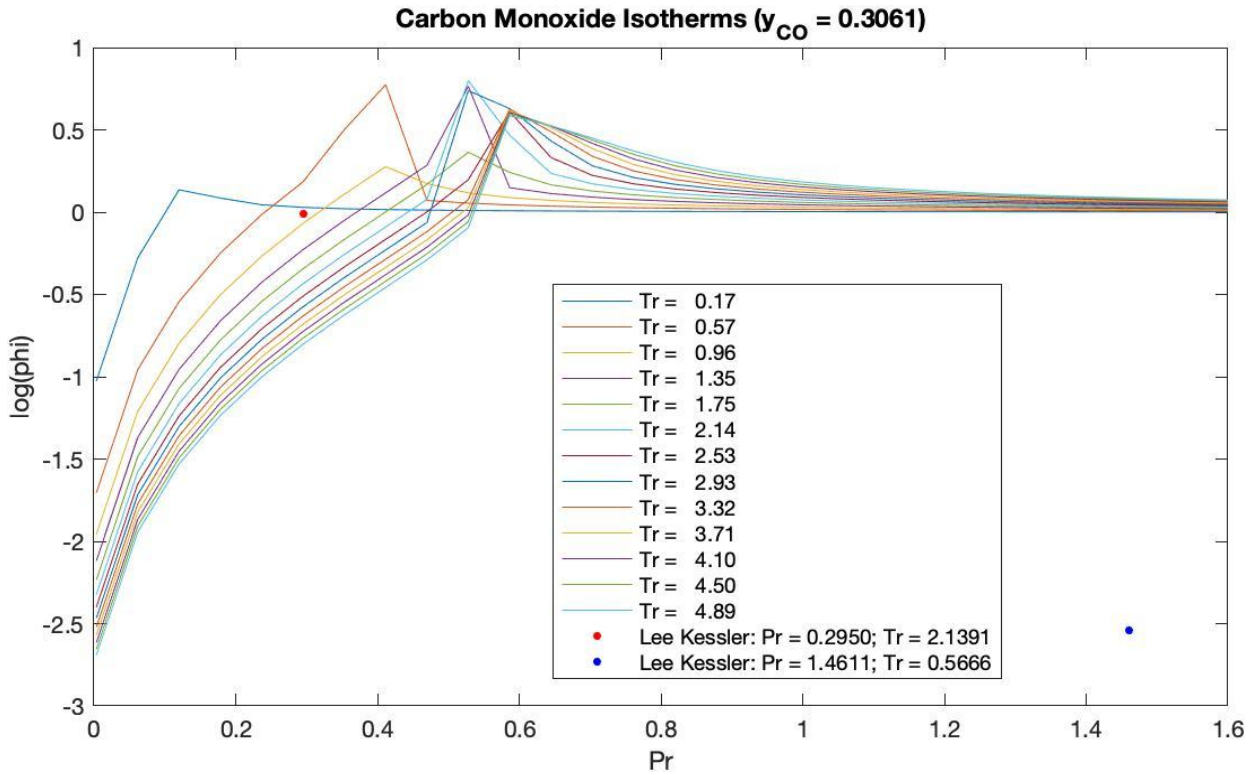

Figure 1: $\log\phi_{CO}$ vs P_r at y_{CO} = 0.3061 (EOS & Lee Kesler)

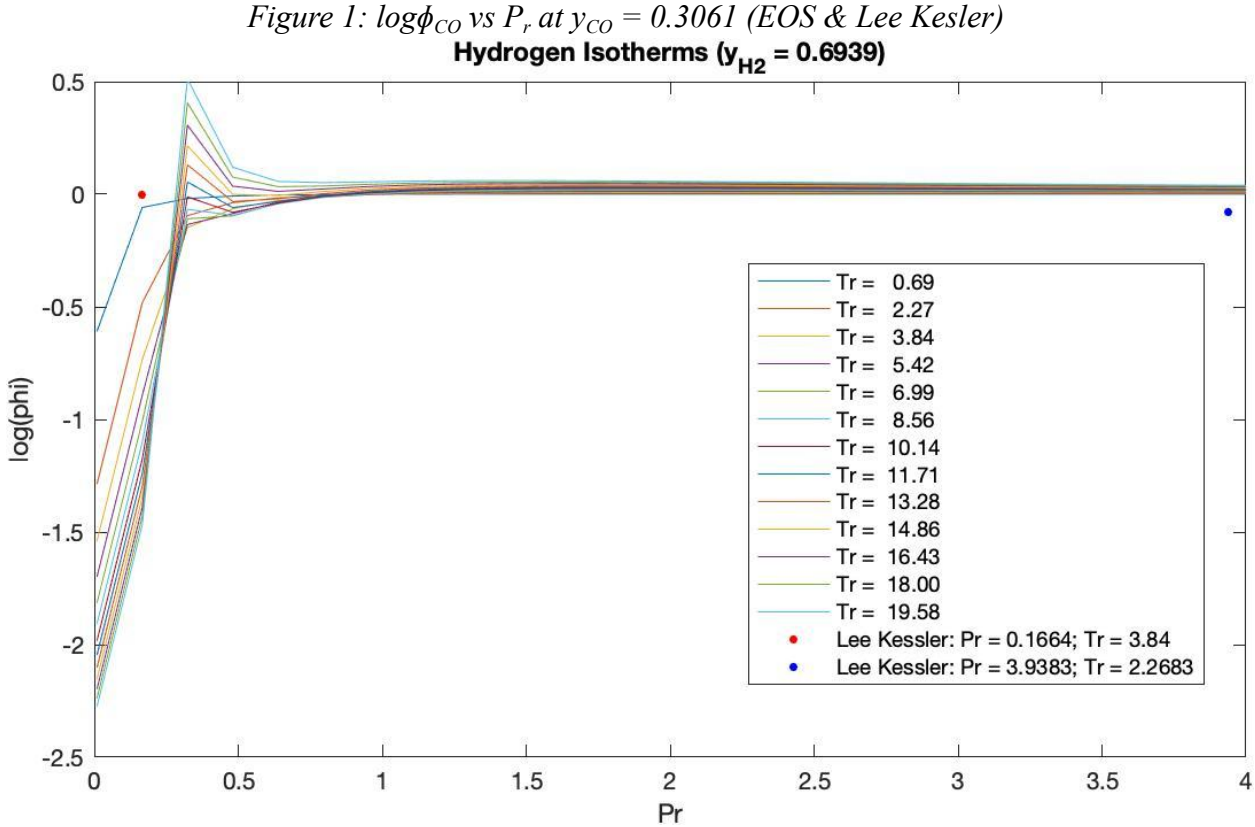

Figure 2: $\log\phi_{H2}$ vs P_r at y_{H2} = 0.6939 (EOS & Lee Kesler)

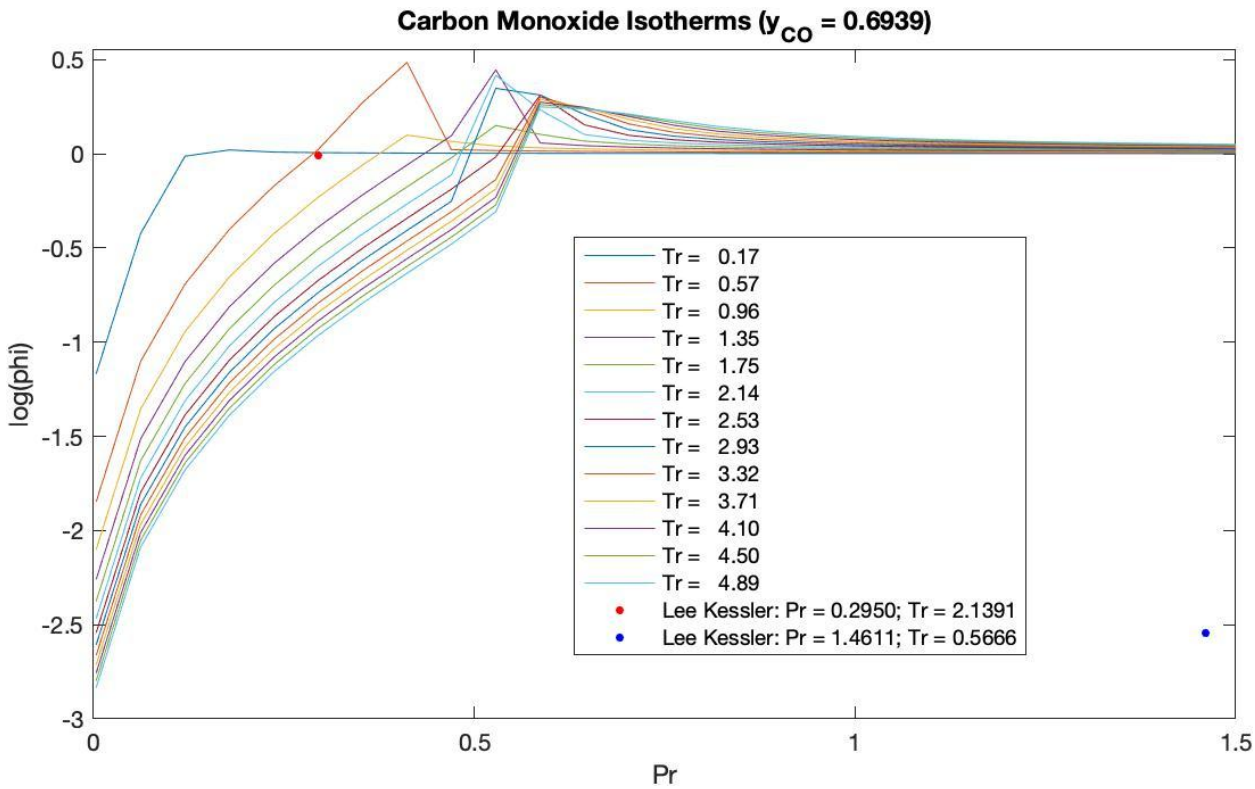

Figure 3: $\log\phi_{CO}$ vs P_r at y_{CO} = 0.6939 (EOS & Lee Kesler)

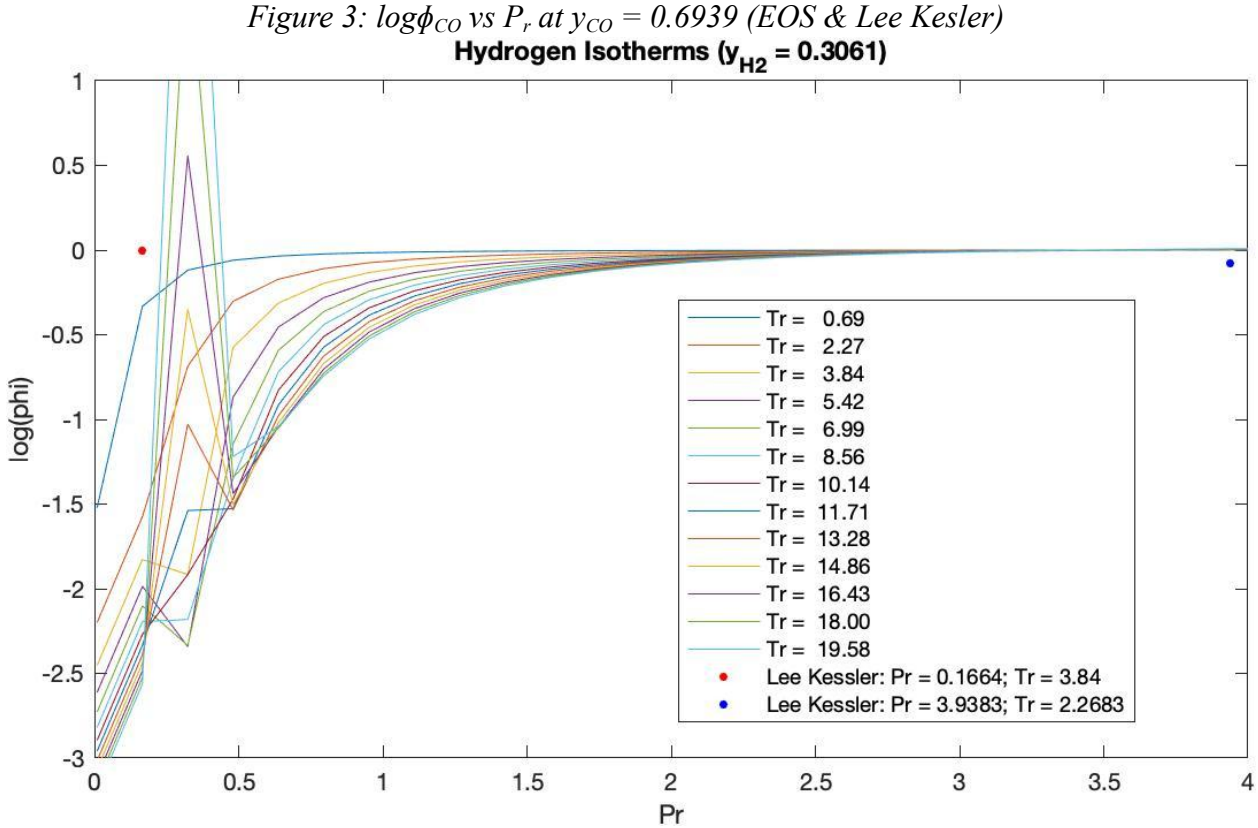

Figure 4: $\log\phi_{H2}$ vs P_r at y_{H2} = 0.3061 (EOS & Lee Kesler)

The CO at both compositions generally peaked at P_r values between 0.4 and 0.6 for all temperatures. At higher pressures, $log(\widehat{\phi})$ asymptotes at 0. For the Lee Kesler data, the $log(\phi)$ generated for ideal conditions (red dot) is consistent with that of the isotherms generated from the modified VdW EOS. However, $log(\phi)$ generated for non-ideal conditions (blue dot) deviates significantly from the VdW EOS.

The H_2 curves peak at P_r values between 0.25 and 0.4 and $log(\widehat{\phi})$ again asymptotes at 0 for higher pressures. For the Lee Kesler data, the $log(\phi)$ generated for both ideal (red) and non-ideal (blue) conditions are consistent with the isotherms from the modified VdW EOS. This data is expected for H_2; due to its small size and single electron, the molecule will behave nearly ideal at most conditions.

Changing Temperature

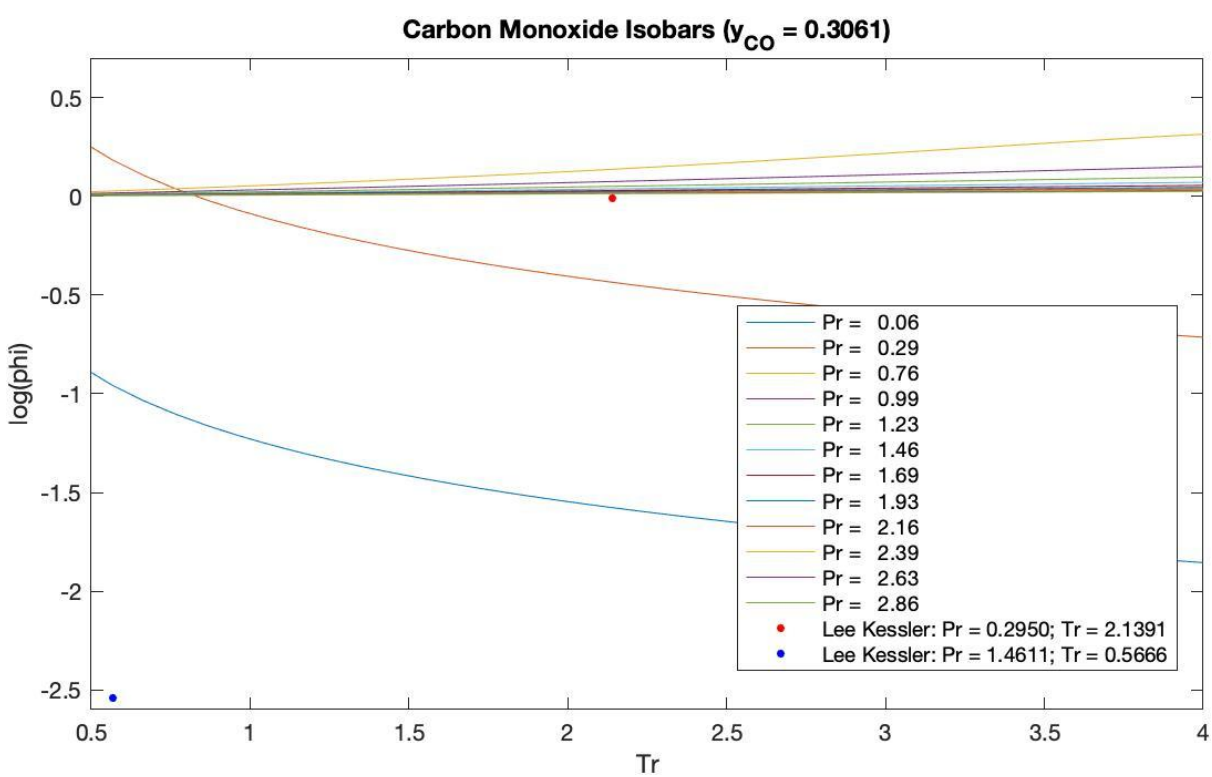

Figure 5: $log\phi_{CO}$ vs T_r at y_{CO} = 0.3061 (EOS & Lee Kesler)

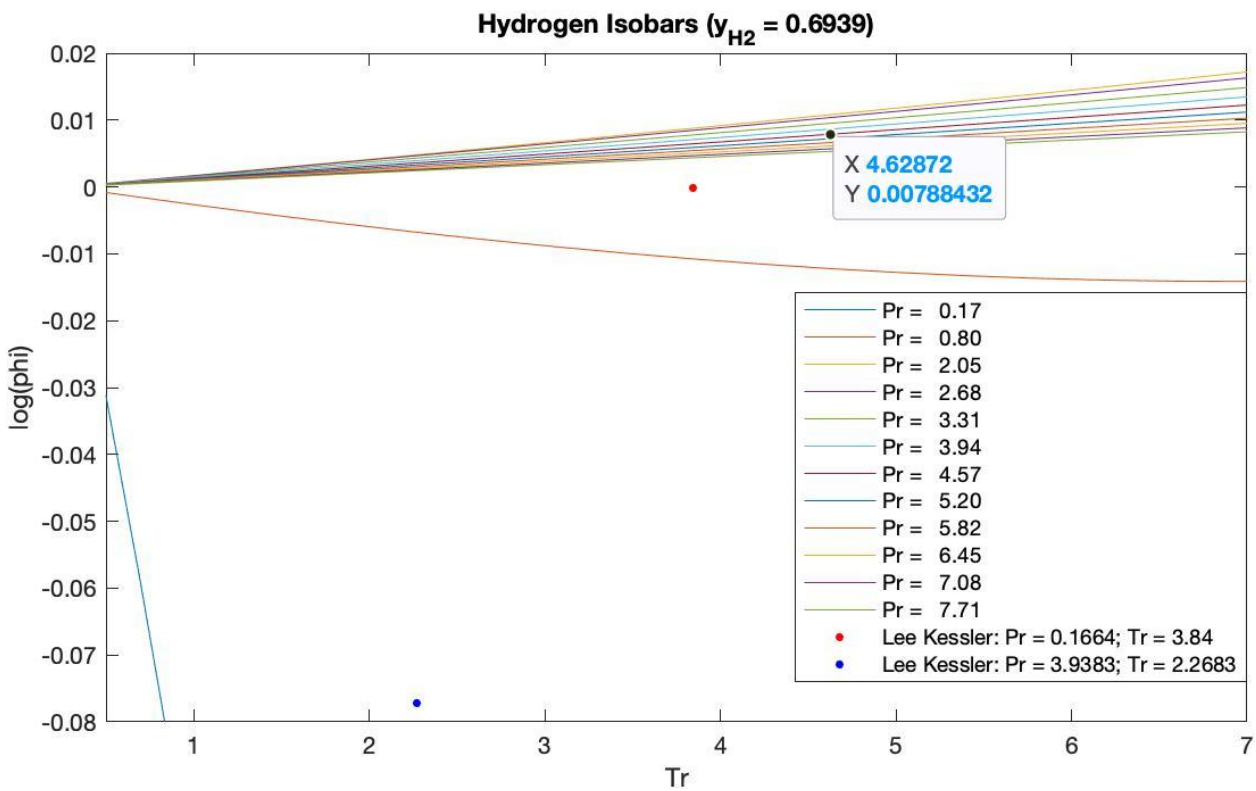

**Figure 6: $\log\phi_{H2}$ vs T_r at y_{H2} = 0.6939 (EOS & Lee Kesler)*

**For this graph, the scale of $\log(\phi)$ is very small in order to properly see the relationship between $\log(\phi)$ and temperature. Therefore, the differences between the Lee-Kesler points and the graph may look amplified.*

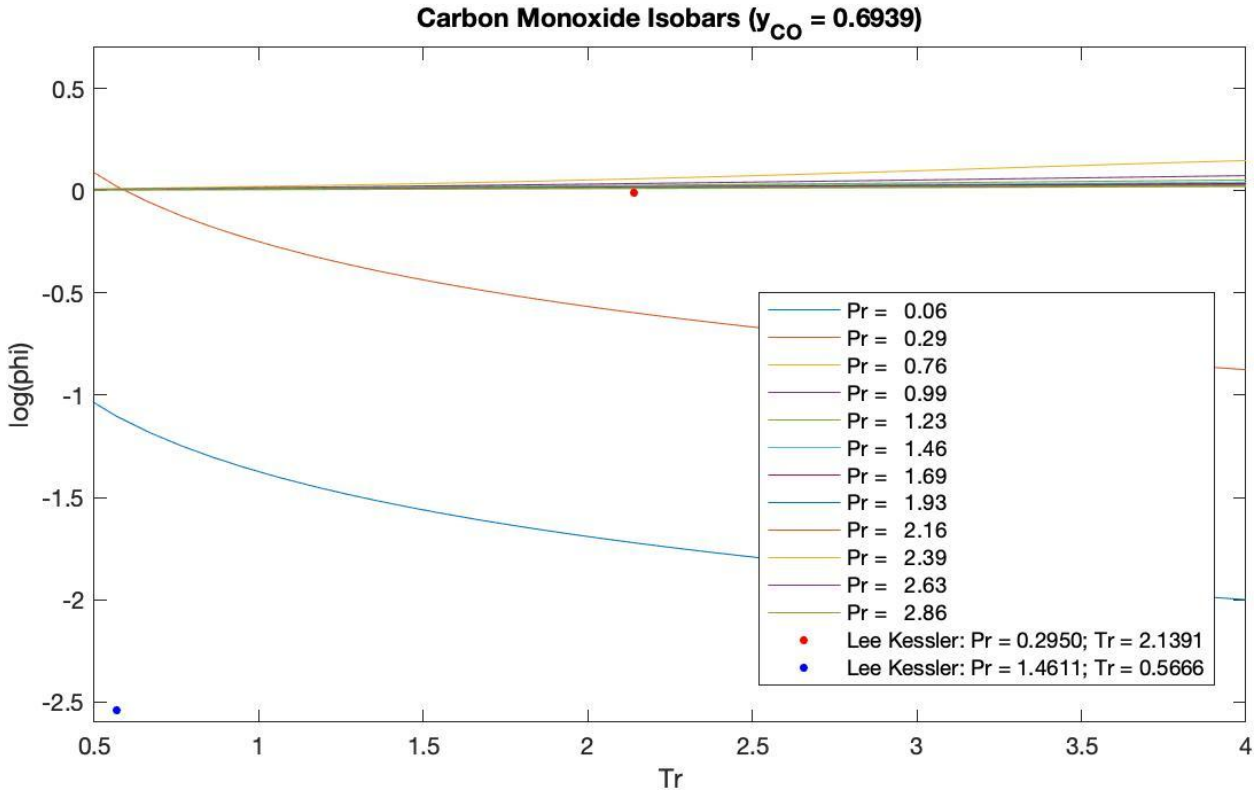

Figure 7: $\log\phi_{CO}$ vs T_r at y_{CO} = 0.6939 (EOS & Lee Kesler)

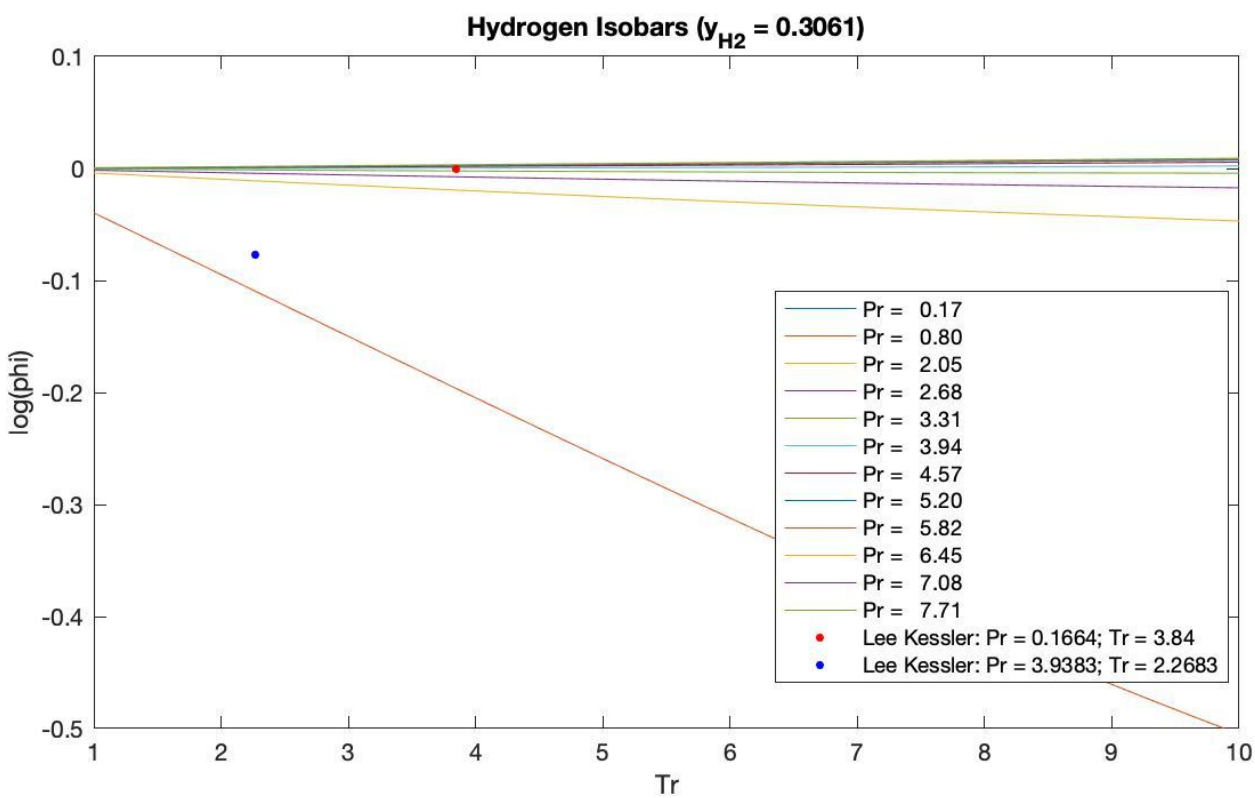

Figure 8: $\log\phi_{H2}$ vs T_r at y_{H2} = 0.3061 (EOS & Lee Kesler)

For Lee Kesler data for CO, the $log(\phi)$ generated for ideal (red) is consistent with the isobars from the modified VdW EOS. However, non-ideal (blue) deviates from the isobar generated from the modified VdW EOS.

For Lee Kesler data for H_2, the $log(\phi)$ generated for both ideal (red) and non-ideal (blue) conditions are consistent with the isobars from the modified VdW EOS. This data is expected for H_2; due to its small size and single electron, the molecule will behave nearly ideal at most conditions.

Changing Composition

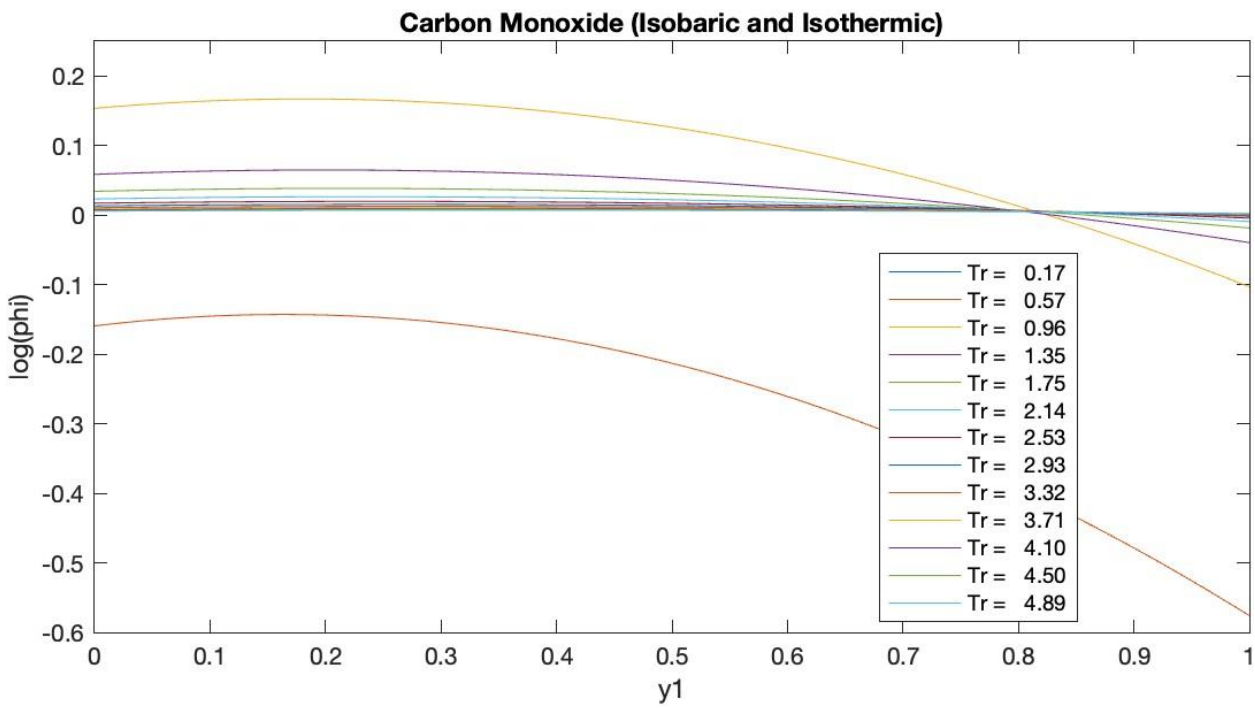

Figure 9: $log\phi_{CO}$ vs y_{CO} at 2.2542 x 10^6 Pa

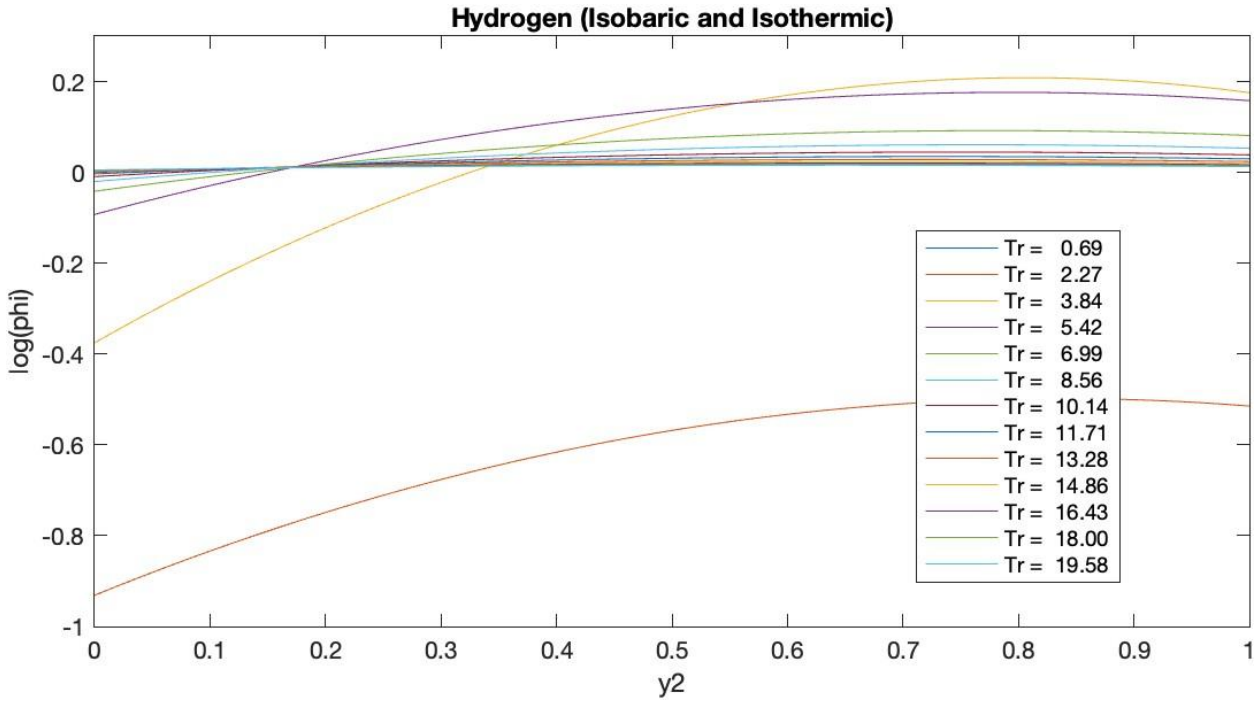

Figure 10: $\log\phi_{H2}$ vs y_{H2} at 2.2542 x 10^6 Pa

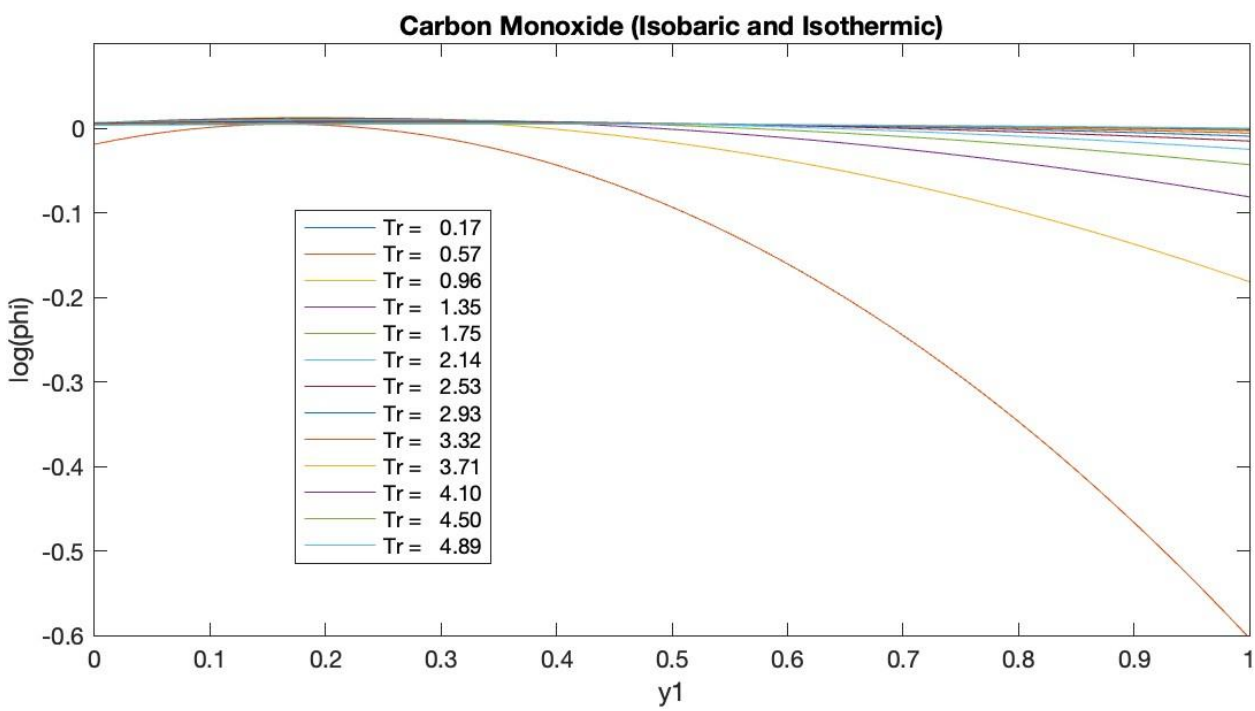

Figure 11: $\log\phi_{CO}$ vs y_{CO} at 5.107918 x 10^6 Pa

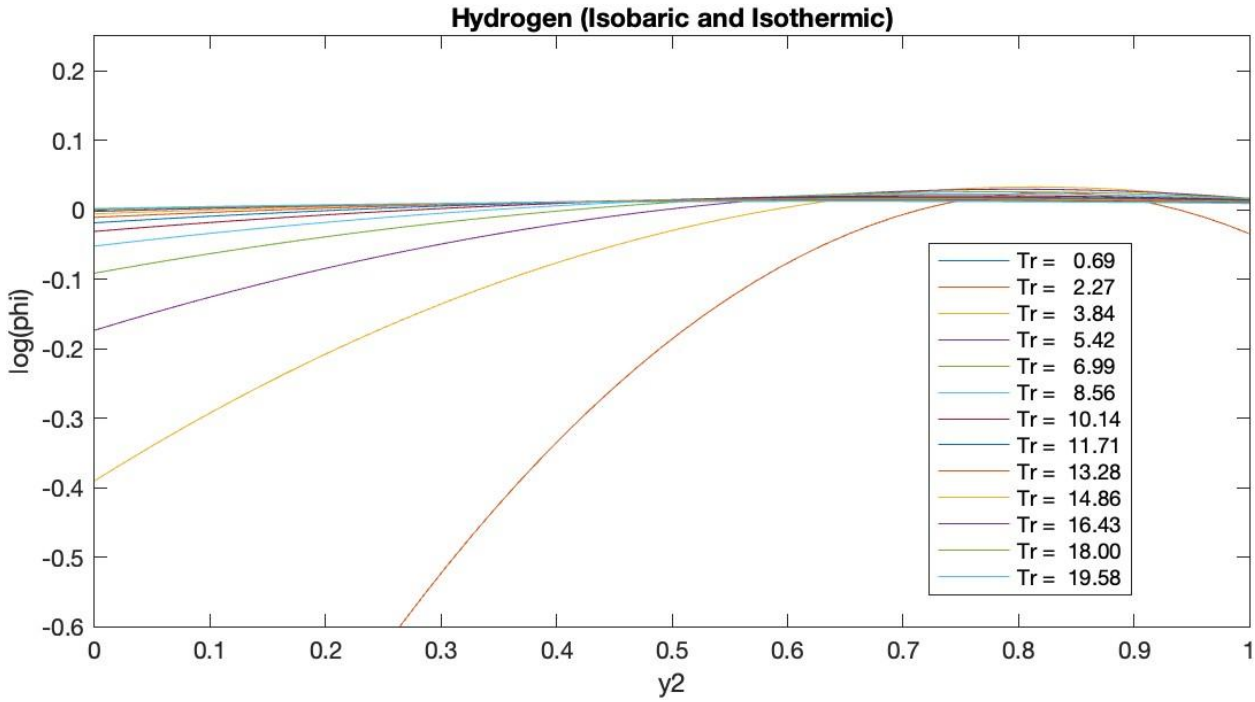

Figure 12: $log\phi_{H2}$ vs y_{H2} at 5.107918 x 10^6 Pa

The CO composition curve at pressure of 2.2542 x 10^6 Pa shows that it asymptotes to 0 when the mixture consists purely of CO (at composition 1), except at some low temperature value. The CO composition curve at pressure of 5.107918 x 10^6 Pa shows that as the composition of CO nears 1, $log(\phi)$ negatively diverges from 0.

The H_2 composition curve at pressure of 2.254 x 10^6 Pa and 5.107917 x 10^6 Pa shows that $log(\phi)$ asymptotes near 0 as the mixture approaches H_2 composition of 1. This suggests that H_2 behaves similarly to ideal gas, due to its small size.

<u>*Discussion*</u>

From our graphs, we can see that across a wide range of temperatures, pressures, and compositions, hydrogen is a gas that behaves ideally. This means that in most environments–even in extreme conditions–it will not deviate significantly from ideal behavior. With this knowledge, hydrogen could be used in a chemical process where you are concerned about not being able to control the conditions. For example, if you wanted to analyze a

component's behavior within a binary mixture at non-ideal conditions. Since one of the two components is hydrogen, most of the deviations from ideality can be attributed to the second component. This can be a useful means of isolating a specific component's mix properties at different ranges of conditions.

Information about the nature of the binary mixture can be learned from looking at the sign (positive or negative) and magnitude of $log(\phi)$ across our ranges of pressure, temperature, and composition. If $log(\phi) < 0$ (negative), fugacity is less than the pressure, and thus attractive forces dominate. If $log(\phi) > 0$ (positive), fugacity is greater than the pressure, and thus repulsive forces dominate. Using this criteria, we can conclude that: at very low reduced pressures (about [0, 0.4]), attractive forces dominate the mixture. However, as pressure increases above this point, repulsive forces begin to dominate for a short range of pressures until it eventually levels back to neutral (as the phase begins to transition to liquid). For most of the range of changing temperatures, behavior of the mixture remains constant. There are a few combinations of conditions that lead to attractive forces dominating, but for the most part the mixture is neutral (acts ideally). From compositions of y_i = [0, 0.8], the forces are relatively neutral, but as the composition increases past this, attractive forces begin to dominate in the mixture. This data is further analyzed in the <u>Conclusion</u> section

Conclusion

While analyzing our data, it must be kept in mind that when $log(\phi) = 0$, $\phi = 1$. Furthermore, this occurs when fugacity ≈ pressure. This relationship means that a component is acting ideally. Incorporating this into our research, we can see from our data (graphs) that an increase in ideal behavior is positively correlated with a decreasing reduced pressure. Once reduced pressure reaches around 0.5, the component begins to stray very far from ideality. This trend reverses when the reduced pressure reaches values around 1 and above, for this is the point when the gas begins to phase change to liquid and the mixture becomes more consistent with that of an ideal mixture. Furthermore, ideal behavior is positively correlated with increased temperature and increased composition (mole fraction: as a mixture component comes closer to pure).

Looking specifically at the relationship of $log(\phi)$ and H_2, we can extrapolate that in most conditions, hydrogen acts ideally. This can be inferred from the fact that you must be very zoomed in on the graphs to see any deviations of $log(\phi)$ from 0. More specifically, this conclusion comes from the following observations of each set of graphs: in the *Changing Pressure* graphs, aside from a small deviation at very small reduced pressures, $log(\phi)$ of hydrogen goes to 0 for a majority of the graph. In the *Changing Temperature* graphs, $log(\phi)$ of hydrogen is almost exactly 0 for the entire range of conditions observed in the project (at y_{H2} = 0.6939, the graph had to be zoomed in to a range of [-0.08 0.02] to even see any trends/deviations among different conditions). In the *Changing Composition* graphs, as the composition of H_2 gets closer to 1, $log(\phi)$ approaches and remains very close to 0. This means that the more H_2 present in the mixture (where it will begin dominating the system's behavior), the more ideal it becomes.

From this analysis, we can further infer that the Lee-Kesler Equation of State is not accurate for binary mixtures at non-ideal conditions. This can be seen in the *Changing Pressure* and *Changing Temperature* sets of graphs by looking at the second, non-ideal point (represented by a blue dot). For both CO and H_2, we can see that the red, ideal point falls near-perfectly in line with the Van der Waals equation of state value (which accounts for intermolecular forces in a mixture), however, the non-ideal point is significantly skewed. Once again taking the relative scales of each graph into consideration, we can see that this deviation is exacerbated with CO, as opposed to H_2 where the difference is less pronounced. Since we previously concluded that hydrogen tends to act ideally across most ranges of conditions, we can reason that deviations in the Lee-Kesler equation of state's accuracy are correlated with an increase in non-ideal behavior of a species.

Works Cited

Guilera, J., Díaz-López, J. A., Berenguer, A., Biset-Peiró, M., & Andreu, T. (2022). Fischer-Tropsch synthesis: Towards a highly-selective catalyst by lanthanide promotion under relevant CO2 syngas mixtures. *Applied Catalysis. A, General*, *629*, 118423-. https://doi.org/10.1016/j.apcata.2021.118423.

Mahmoudi, H., Mahmoudi, M., Doustdar, O., Jahangiri, H., Tsolakis, A., Gu, S., & LechWyszynski, M. (2017). A review of Fischer Tropsch synthesis process, mechanism, surface chemistry and catalyst formulation. *Biofuels Engineering*, *2*(1), 11–31. https://doi.org/10.1515/bfuel-2017-0002.

Stolecka, K., & Rusin, A. (2020). Analysis of hazards related to syngas production and transport. *Renewable Energy*, *146*, 2535–2555. https://doi.org/10.1016/j.renene.2019.08.102.

Sun, S., Lv, Z., Qiao, Y., Qin, C., Xu, S., & Wu, C. (2021). Integrated CO2 capture and utilization with CaO-alone for high purity syngas production. *Carbon Capture Science & Technology*, *1*, 100001-. https://doi.org/10.1016/j.ccst.2021.100001.

Thomson, R., Kwong, P., Ahmad, E., & Nigam, K. D. P. (2020). Clean syngas from small commercial biomass gasifiers; a review of gasifier development, recent advances and performance evaluation. *International Journal of Hydrogen Energy*, *45*(41), 21087–21111. https://doi.org/10.1016/j.ijhydene.2020.05.160.